HOKKAIDO UNIVERSITY

Title	Thermal accumulation effect in three-dimensional recording by picosecond pulses
Author(s)	Juodkazis, Saulius; ヨードカジス, サウルース; Misawa, Hiroaki et al.
Citation	APPLIED PHYSICS LETTERS, 85(22), 5239-5241 https://doi.org/10.1063/1.1829799
Issue Date	2004-11
Doc URL	https://hdl.handle.net/2115/5897
Rights	Copyright © 2004 American Institute of Physics
Type	journal article
File Information	APL85-22.pdf

Thermal accumulation effect in three-dimensional recording by picosecond pulses

Saulius Juodkazis and Hiroaki Misawa[a]

CREST-JST and Research Institute for Electronic Science, Hokkaido University, CRIS Bldg. N21-W10, Sapporo 001-0021, Japan

Igor Maksimov[b]

Satellite Venture Business Laboratory, The University of Tokushima, 2-1 Minamijosanjima 770-8506, Tokushima, Japan

In-bulk recording without cracking in borosilicate glass by high repetition rate (80 MHz) 12 ps pulses at 355 nm wavelength is demonstrated and discussed. The theoretical model of a "hot-line" scan and thermal accumulation qualitatively well describes the experimental results. The analytical expression of a thermally induced stress was obtained. © *2004 American Institute of Physics.* [DOI: 10.1063/1.1829799]

Recent advances in microfabrication, in which ultrafast lasers with pulse durations of less than 1 ps are implemented, show the potential ability to record sub-μm structures inside transparent materials.[1,2] The nonlinear mechanism of absorption allows the photomodification to be localized within the volume[2] or on the surface[3] with a cross section smaller than the wavelength, λ. The diffraction limit of the focusing optics can be overcome. However, for some three-dimensional (3D) microstructuring tasks, a high repetition rate (over 200 kHz) is required to achieve partial softening/melting of glass.[4] Obviously, longer pulses (from picoseconds to nanoseconds) could be considered for this type of recording, however, they usually cause crack formation in glass. Recently, it was demonstrated that brittle materials can also demonstrate a ductile response before onset of crack formation at a specific crossover length of order 10 nm in glass.[5] Control of the local temperature and its distribution inside transparent materials at the focus allows one to tune a thermal stress for a desired application, e.g., a 3D dicing (a controlled cleaving) would require a controlled crack propagation, while the optical memory and waveguide recording would benefit from prevention of the crack formation by material softening/melting.

The aim of this work was to investigate the effect of thermal accumulation on 3D laser recording by 12 ps duration, 355 nm wavelength pulses at a high (80 MHz) repetition rate inside glass. The experimental results are compared with those of theoretical modeling.

A Vanguard (Spectra Physics) laser was used for 3D recording inside borosilicate slide glass (Corning 2947). Recording was carried out by beam scanning with galvano mirrors at a constant speed of 5–10 cm/s using θ-lens focusing, which fixed the focal depth along the line of recording inside the 1-mm-thick samples (aimed at the center). The pulse duration was 12 ps, the repetition rate 80 MHz, the maximum pulse energy 50 nJ, and the wavelength 355 nm. In-bulk laser fabrication is possible at this wavelength because the main absorption mechanism is a nonlinear two-photon absorption (TPA). The TPA coefficient of slide glass $\beta = 25 \pm 7$ cm/GW was directly measured at 355 nm using by the transmission method applicable when linear absorption is negligible.[6] The edge of glass absorption was at approximately 320 nm wavelength where the decadic optical density (OD) > 0.1 for a 1-mm-thick glass; while the linear absorption coefficient at 355 nm was only $\alpha_0 = 0.47$ cm^{-1}.

For recording, we used focusing defined by f-number $(f_\#) = 10$, at which a cost-efficient diffraction-limited performance of lens can be achieved. For a Gaussian pulse, the diameter of the focal spot is $d = B\lambda f_\#$,[7] where $f_\# = f/a$ is defined by the lens focal length, f, and the aperture of the beam, a. The constant B depends on the intensity level at which the diameter is measured. In our experiments, we use an $f \simeq 100$ mm lens for which the focal spot diameter at full width half maximum was $d_{1/2} = 4$ μm ($d_{1/e^2} = 6.5$ μm).

The axial extent of the focus, the depth of focus (DOF), is defined by the length at which the waist of a Gaussian beam increases by 5%, i.e., DOF $\simeq 0.64\pi d_{1/e^2}^2/\lambda = 239$ μm. Thus, the axial extent of the beam was much larger than the diameter at focus. In addition, the axial intensity decays as $|z|^{-2}$ for a Gaussian beam/pulse, while the lateral intensity decreases exponentially; here, z is the axial coordinate. Hence, to model sample heating at the focal region, it is appropriate to consider the linear focus even when self-focusing, which has a threshold at 2–3 MW for glasses,[8] is avoided. The maximum power per pulse was 4.2 kW in our experiments, so that we did not have to consider the effects of self-focusing.

Next, let us consider the stress generated by heating and its accumulation. A two-dimensional model is implemented, in which a heat source delivers power q (W) to a strip of length d (a linear excitation through the entire thickness of the sample); the strip is scanned along the x axis at velocity v [Fig. 1(a)]. The distribution of the corresponding temperature, T, is the solution of a temperature diffusion equation:[9]

$$c\frac{\partial T}{\partial t} - \kappa\Delta T = q\,\delta(\boldsymbol{x} + \boldsymbol{v}t), \tag{1}$$

where c (J K^{-1} m^{-3}) is the specific heat capacity density, κ (W m^{-1} K^{-1}) is the thermal conductivity, and δ marks the

[a]Author to whom correspondence should be addressed; electronic mail: misawa@es.hokudai.ac.jp
[b]On leave from the Physics Faculty, Nizhny Novgorod University, 23 Gagarin Ave., Nizhny Novgorod 603000, Russia.
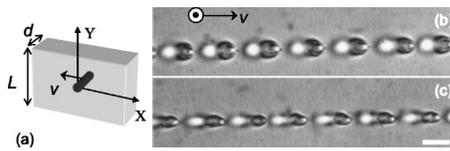
FIG. 1. (a) Geometry of a hot-line scanning experiment, where v is the velocity of a linear heat source. Sample's lateral dimensions are much larger than its thickness, $L \gg d$. (b) and (c) Optical images of 3D recording by 12 ps pulses of 355 nm wavelength at an 80 MHz repetition rate inside glass at $f_\# = 10$ focusing; the pulse energy was 40 nJ. The beam scanning speed was 5 cm/s (b) and 10 cm/s (c). Scale bar 50 μm. Directions of irradiation and beam scanning are marked in (b).

delta function. The analytical solution of this equation is:[9]

$$T(x, y=0) = \frac{q}{2\pi d\kappa} e^{(x/\ell)} \mathbf{K}_0(|x|/\ell), \qquad (2)$$

where $\ell = \kappa/(cv)$ is the length of thermal diffusion and $\mathbf{K}_0$ is the modified Bessel function of the first kind and 0–th order. This temperature distribution causes stress to build up, which can be found from:

$$\sigma_y(x) = \mu(1+\nu)\alpha\left[\int_0^1 T(x,\xi)d\xi - T(x)\right], \qquad (3)$$

with μ (Pa) being the shear modulus, α (K^{-1}) is the linear thermal expansion coefficient, and ν is the Poisson ratio. Finally, stress is given by

$$\sigma_y(x) = \sigma_{max}\left(e^{\frac{x}{\ell}}\mathbf{K}_1\left(\frac{|x|}{\ell}\right)\text{sign}(x) - \frac{\ell}{x}\right), \qquad (4)$$

where $\sigma_{max} = q\mu\alpha(1+\nu)/(2\pi d\kappa)$ is the maximum stress defined via material parameters for a given heating power q, and $\mathbf{K}_1$ is the modified Bessel functions of the first kind and 1-st order. If stress exceeds the critical value, the tensile strength of material T_S (Pa), fracturing ensues. For cleaving applications, the fracture toughness K_I (Pa$\sqrt{\text{m}}$) should be considered instead. In that case, once the critical value surpasses $K_I \equiv \sigma_{max}\sqrt{\ell} > K_{IC}$, cleaving is likely.

The formulae given is the exact analytical solution, which allow one to determine the relevant importance of parameters for different 3D laser processing applications: Dicing, waveguide, and optical memory recording in dielectric materials by focused high-intensity irradiation. This analytical model is solved for the laser excitation by a moving heat source whose lateral cross section is the δ-function. In actual experiments, the finite spot size should be considered and numerical methods should be implemented to calculate local temperature and its spatial distribution. The influence of the finite focal spot size is discussed next.

The maximum temperature rise per single pulse can be evaluated for the maximum irradiance of 3.4×10^{10} W/cm^2 at focus, when the absorption coefficient is $\alpha(I) = \alpha_0 + \beta I \simeq 850$ cm^{-1}. For a typical glass thermal capacity of $c_p = 880$ J/(kg K) and mass density 2.2 g/cm^3, the temperature change within the absorption volume is 179 K; here, the absorption volume is calculated as of a cylinder whose diameter is equal to the diameter of beam at focus and height is $1/\alpha(I)$.

The heat accumulation at the focal spot is effective in glasses due to their low thermal diffusivity. That of a borosilicate glass is typically $\chi = 4.6 \times 10^{-3}$ cm^{-2}/s (Pyrex), here, $\chi = \kappa/c_s$, where c_s is the specific heat capacity [J/(K m^3)].

For example, the thermal conductivity of sapphire is 37 times higher than that of Pyrex $\kappa = 1.13$ W/(m K). The effective cooling time defined as $t_c = d^2/\chi$ for the spot of $d = 4$ μm diameter yielding in the cooling constant of 33 μs. This is larger than the 12.5 ns interval between pulses, and the multipulse irradiation is expected to increase the temperature at focus. It is instructive to evaluate the number of pulses that accumulate over the spot size at a given scanning speed, v. For $v = 5$ cm/s, number of pulses accumulated over the spot diameter at a repetition rate of 80 MHz is 6.3×10^3, while the length of thermal diffusion is $\ell_d \equiv \chi/v = 9.3$ μm.

The stationary solution for the temperature field along propagation of the hot line predicts the temperature rise ahead of the heating point at $x = 0$ as can be easily assessed from Eq. (2). For an actual pulsed laser irradiation, this would mean that material is preheated as discussed above. However, the heat source in Eq. (2) is modeled as a continuous wave (cw) with a δ-function cross section, hence, rendering the results being only qualitative.

It was confirmed by optical inspection that cracks larger than approximately one-half of the radius at focus were not present inside slide glass after recording. This suggests that temperatures in the region of 500–600 °C were probably achieved at the focus (e.g., the softening point of Pyrex is 560 °C) and crack formation was prevented.

Figures 1(b) and 1(c) show the transmission images of lines recorded inside the borosilicate slide glass at two different scanning speeds. Surprisingly, the resulting lines appear to be comprised of dots even though the beam scanning by galvanic mirrors was smooth and constant. The length between dots depended only slightly on the scanning speed, while the width of the recorded line depended on the scanning speed as $\sqrt{1/v}$, as would be expected with the diffusion-controlled process. Based on the discussion above, we can present the following scenario of line recording in slide glass. A high-repetition rate irradiation increases the temperature at the focus via nonlinear absorption and accumulation till the light-induced damage threshold (LIDT) and then the dielectric breakdown ensued. The dotted-line type damage resulted from the temperature dependence of the LIDT.

The temperature dependence of LIDT is closely correlated with the temperature dependence of the linear expansion coefficient, α_ℓ, in glass as we reported earlier.[10] For example, heating up to 100–200 °C reduces the LIDT value twice in silica.[10] Pyrex, for example, was designed for the linear dependence of α_ℓ on the temperature (the same as in Si) up to a strain point at 510 °C; hence, the temperature dependence of LIDT is expected to depend on temperature in a similar way. If heat accumulates, an increasing local temperature will reduce the LIDT value until the breakdown point is reached for a given irradiance. The optical breakdown, i.e., an ionization of the focal volume, was observed as a white light of plasma emission during scanning at the appearance frequency, which corresponded to the period of the dotted line in Fig. 1 corroborating the proposed model. The plasma emission was not observed when the laser beam was scanned faster than 50 cm/s at the same pulse energy as shown in Fig. 1.

The region of breakdown becomes a strong optical scatterer due to the changed structural morphology, hampering the delivery of subsequent pulses to the focal region. This reduces the local temperature at the irradiation spot. After the
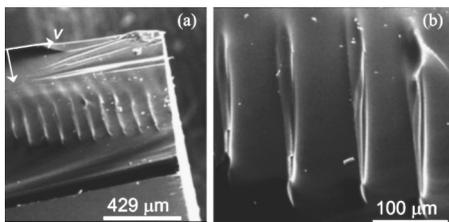
FIG. 2. (a) SEM image of slide glass cleaved along the recorded line. Recording conditions were the same as for the sample shown in Fig. 1(c). (b) Close-up view of (a).

scanning beam passes the breakdown area, heat begins to accumulate again and the processes repeats. A side-view scanning electron microscope (SEM) image of the recorded line after a slide glass was cleaved showed a linear morphology at the breakdown points (Fig. 2). The dimensions and shape of the photomodified regions corroborate the proposed model of recoding by heat accumulation and optical breakdown.

If needed, highly localized nonhomogeneous heating can be used to cleave/dice dielectrics or to record corresponding refractive index profiles. Figure 3 shows the calculated [by Eq. (4)] distribution of toughness along the scanned line for the linear heat source moving in glass (Pyrex) at different speeds. Simulations were carried out using stress expression [Eq. (4)] for Pyrex parameters without taking into account the temperature dependence of LIDT. For a constant heat load of 15 W (by a δ-function heat source), the 2.5 cm/s scanning should cause a Pyrex plate to crack, while at higher speeds the stress becomes increasingly localized. As one can see (Fig. 3), the proper choice of irradiation (heating) fluence and scanning speed allows the creation of a highly localized temperature-caused stress inside glass without reaching the
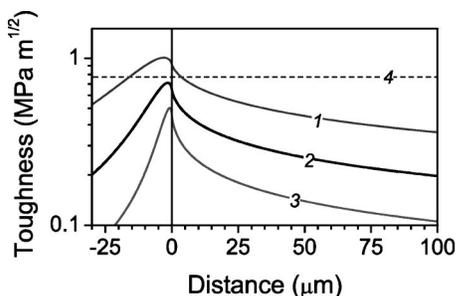

FIG. 3. Toughness K_I vs coordinate (in the moving system of coordinates) at different scanning speeds of $v=2.5$ (1), 5 (2), and 10 cm/s (3), for a $q=15$ W heat source, when the source is $d=1$ mm long. The other parameters are typical for Pyrex: $\mu=26$ GPa, $\alpha=3.25\times10^{-6}$ K^{-1}, $\nu=0.2$, $c=2.44\times10^{6}$ J K^{-1} m^{-3}, and $\kappa=1.13$ W m^{-1} K^{-1}. The dashed line shows the fracture toughness of Pyrex glass $K_{IC}=0.77$ MPa$\sqrt{m}$ (4).

mechanical failure point. Simulation of heating by the linear heat source using Eq. (4) cannot produce quantitative fit with experimental data since the lateral dimensions of the heat source are finite and cannot be modeled by δ-function. Hence, the heat load cannot be directly compared with the real recording (Fig. 3). However, Eq. (4) describes qualitatively well the phenomenon of a thermal stress control inside transparent materials and can be useful to simulate 3D processing of transparent materials. The proposed model can also describe fabrication by nondiffracting Bessel beams/pulses.[11,12] The main virtue of the model is that the analytical expression was obtained.

In conclusion, we have demonstrated crack-free recording inside borosilicate slide glass by 12 ps pulses of 355 nm wavelength at 80 MHz repetition rate. The mechanism of recording is explained by the heat accumulation at focus, leading to dielectric breakdown without crack formation in a softened material around the irradiated volume. The heat-generated stress inside glass can be used to control spalling and dicing of transparent materials. High-temperature regions can be spatially localized by controlling the pulse energy and scanning speed. This method could be also used for recording of refractive index changes inside transparent materials.

[1]C. B. Schaffer, A. O. Jamison, and E. Mazur, Appl. Phys. Lett. **84**, 1441 (2004).

[2]S. Juodkazis, A. V. Rode, E. G. Gamaly, S. Matsuo, and H. Misawa, Appl. Phys. B: Lasers Opt. **77**, 361 (2003).

[3]E. Vanagas, I. Kudryashov, D. Tuzhilin, S. Juodkazis, S. Matsuo, and H. Misawa, Appl. Phys. Lett. **82**, 2901 (2003).

[4]C. B. Schaffer, A. Brodeur, J. F. Garca, and E. Mazur, Opt. Lett. **26**, 93 (2001).

[5]C. Marliere, S. Prades, F. Celarie, D. Dalmas, D. Bonamy, C. Guillot, and E. Bouchaud, J. Phys.: Condens. Matter **15**, S2377 (2003).

[6]M. Miwa, S. Juodkazis, T. Kawakami, S. Matsuo, and H. Misawa, Appl. Phys. A: Mater. Sci. Process. **73**, 561 (2001).

[7]A. E. Siegman, *Lasers* (University Science Books, Mill Valley, CA, 1986).

[8]A. A. Zozulya, S. A. Diddams, and T. S. Clement, Phys. Rev. A **58**, 3303 (1998).

[9]V. Parton and E. M. Morozov, *Mechanics of Elastic–Plastic Fracture* (Nauka, Moscow, 1984).

[10]S. Juodkazis, A. Marcinkevicius, M. Watanabe, V. Mizeikis, S. Matsuo, and H. Misawa, Proc. SPIE **4347**, 212 (2001).

[11]A. Marcinkevicius, S. Juodkazis, S. Matsuo, V. Mizeikis, and H. Misawa, Jpn. J. Appl. Phys., Part 2 **40**(11A), L1197 (2001).

[12]E. Vanagas, V. Jarutis, S. Juodkazis, V. Mizeikis, I. Kudryashov, S. Matsuo, H. Misawa, and R. Tomašiūnas, Lith. J. Phys. **43**, 243 (2003).